



HAL
open science

Thermal Behaviour of Deep Levels at Dislocations in n-Type Silicon

D. Cavalcoli, A. Cavallini, E. Gombia

► **To cite this version:**

D. Cavalcoli, A. Cavallini, E. Gombia. Thermal Behaviour of Deep Levels at Dislocations in n-Type Silicon. *Journal de Physique III*, 1997, 7 (12), pp.2361-2366. 10.1051/jp3:1997103 . jpa-00249724

HAL Id: jpa-00249724

<https://hal.science/jpa-00249724v1>

Submitted on 4 Feb 2008

HAL is a multi-disciplinary open access archive for the deposit and dissemination of scientific research documents, whether they are published or not. The documents may come from teaching and research institutions in France or abroad, or from public or private research centers.

L'archive ouverte pluridisciplinaire **HAL**, est destinée au dépôt et à la diffusion de documents scientifiques de niveau recherche, publiés ou non, émanant des établissements d'enseignement et de recherche français ou étrangers, des laboratoires publics ou privés.

Thermal Behaviour of Deep Levels at Dislocations in n-Type Silicon

D. Cavalcoli ⁽¹⁾, A. Cavallini ^(1,*) and E. Gombia ⁽²⁾

⁽¹⁾ INFN and Department of Physics, University of Bologna, viale B. Pichat 6/II, 40127 Bologna, Italy

⁽²⁾ CNR MASPEC Institute, via Chiavari 18/A, 43100 Parma, Italy

(Received 3 October 1996, accepted 21 August 1997)

PACS.61.72.Ff – Direct observation of dislocations and other defects (etch pits, decoration, electron microscopy, X-ray topography, *etc.*)

PACS.61.72.Lk – Linear defects: dislocations, disclinations

PACS.71.20.Mq – Elemental semiconductors

Abstract. — The thermal behaviour of deformation-induced traps in plastically deformed n-type silicon has been investigated *via* Deep Level Transient Spectroscopy. Among the four traps usually detected in plastically deformed silicon only two have been found to survive upon annealing: trap A and trap C located at 0.18–0.23 eV and 0.38–0.43 eV from the conduction band edge, respectively. The last one has been related to dislocations.

1. Introduction

Plastic deformation introduces, besides dislocations, a large amount of point defects that strongly influence the semiconductor electronic properties. Since the annealing process is the most widely used method to decrease the point defect concentration, the study of the thermal behaviour of the traps is of great interest. Several electronic studies of the annealing kinetics of deformation induced states have been reported in literature [1], which, however lead to different conclusions.

The thermal stability of deformation induced defects will be the subject of the present paper. Annealing procedures have been carried out on plastically deformed (PD) Si in order to decrease the point defect contribution and to check for possible modifications of the detected levels. DLTS (Deep Level Transient Spectroscopy) analyses have been performed both on as-deformed and on annealed samples. The results of these investigations have given further insight on the microscopical identification of deformation-induced defects.

2. Experimental Details

High purity, float-zone, n-type, {111} Si single crystals, grown by Wacker Chemitronic with free carrier concentration of 5×10^{13} (phosphorus atoms)/cm³, were used in this study. Details

(* Author for correspondence (e-mail: cavallini@bologna.infn.it)

Table I. — *Details of the deformation and annealing procedures. T_d and t_d are the deformation temperature and time, respectively, τ the resolved shear stress.*

SAMPLE	T_d (°C)	t_d (h)	τ (MPa)
DAT1	650	60	38
DAT3	750	24	25

of the deformation procedure can be found in [2]. The treatment conditions (deformation temperature T_d , duration t_d and resolved shear stress τ) are reported in Table I. The annealing procedure was performed by heating the samples at 850 °C for one hour in forming gas (92% N₂, 8% H₂). In set DAT3 we observed [2] overlapping peaks in the most dislocated samples and clearly resolved peaks in the less dislocated ones, while in the set DAT1 we found detectable DLTS peaks only in the most dislocated samples. Therefore we examined by DLTS before and after annealing the less dislocated samples of DAT3 (dislocation density $N_D = 10^4 \text{ cm}^{-2}$) and the most dislocated ones of DAT1 ($N_D = 10^6 \text{ cm}^{-2}$). After deformation, Schottky diodes (Au dots 1 mm diameter) were prepared on the samples ($2 \times 5 \text{ mm}^2$ wide), while ohmic contacts were realized with Ga-Al alloy on the back surface. Then the samples were analyzed by DLTS. After removal of the diodes the samples were annealed and Schottky diodes realized again in the previous position in order to avoid problems due to the inhomogeneous dislocation distribution, especially in the set DAT1. Further details of the experimental methods employed in this investigation have been described elsewhere [3].

3. Results

DLTS spectra of as-deformed and annealed samples are shown in Figure 1 for the set DAT1 (a) and DAT3 (b), respectively. Here the peaks are labelled A, B, C, D, according to references [3] and [4]. The main features common to both sets are the decrease of the amplitude of most of the observed peaks, the disappearance of levels B and D, and the survival of levels A and C after annealing. Other features differ between the two sets: in DAT1 samples the line C contribution significantly decreases, while in DAT3 it remains almost unchanged, due to the partial annealing occurred during the sample cooling after deformation that reduces the concentration of point defects in as-deformed materials too [2]. The annealing influences also the shape of the peaks: in DAT1 the peak C is made up of two different lines in the as-deformed samples (see also Fig. 3) reducing to a single line after annealing, while in DAT3 peak C is a single line peak both in deformed and annealed samples.

In Figure 2 the thermal emission rates e_n (T^2 -corrected) of A and C levels in as-deformed and annealed samples are plotted as a function of inverse temperature for DAT1 (a) and DAT3 (b) sets, respectively. In DAT1 the line C can be resolved in two contributions (labelled C1 and C2) which reduce to one single line after annealing, while in DAT3 the "finger prints" of lines A and C in the as-deformed samples overlap with those relative to annealed samples. By comparing the Arrhenius plots in Figure 2, line C after annealing could be associated to line C1.

The observed DLTS peaks, as often occurs in PD silicon, are broadened (Fig. 1). They have been analyzed on the basis of the model reported in reference [4], in which prefactor A_{pf} was defined as $A_{pf} = \sigma_n < \nu_{th} > N_{CB} \times \exp\left(\frac{\Delta S}{k}\right)$ with σ_n the majority carrier capture

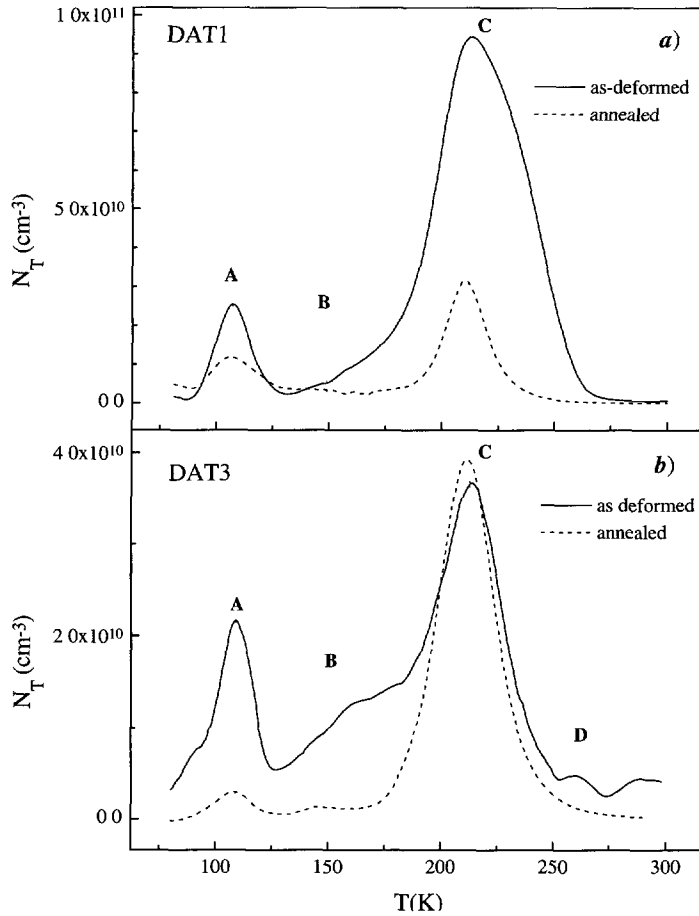


Fig. 1 — Deep Level Transient Spectroscopy spectra before (solid line) and after (dashed line) annealing of a sample (dislocation density $\approx 10^6$ cm⁻²) of the set DAT1 (a) and of a sample (dislocation density $\approx 10^4$ cm⁻²) of the set DAT3 (b) (emission rate. $e_n = 134$ s⁻¹, filling pulse height: $U_p = 0.3$ V, reverse bias. $U_r = 7$ V, filling pulse width. $t_p = 100$ μ s).

cross-section, $\langle \nu_{th} \rangle$ the electron average thermal velocity, N_{CB} the density of states in the conduction band, ΔS the change in entropy due to the emission of an electron from the deep level to the conduction band edge, and k the Boltzmann constant. The activation enthalpies E_a and prefactors A_{pf} were evaluated by fitting the DLTS peaks with the above cited model and from the Arrhenius plots, they are reported in Table II. It is worth noting here the different characteristics of line C in DAT1 set before and after annealing: the peak in as-deformed material could not be fitted with the above cited model, but it was deconvoluted in two peaks C1 and C2 (Fig. 3). On the contrary, after annealing it could be analyzed on the basis of the model as a broadened line C.

Furthermore, from the analysis of the capture kinetics, the level C was found to be associated with a time-dependent potential barrier whose asymptotic value is 0.23 eV, in agreement with the value obtained for the same level in the set DAT3 [2].

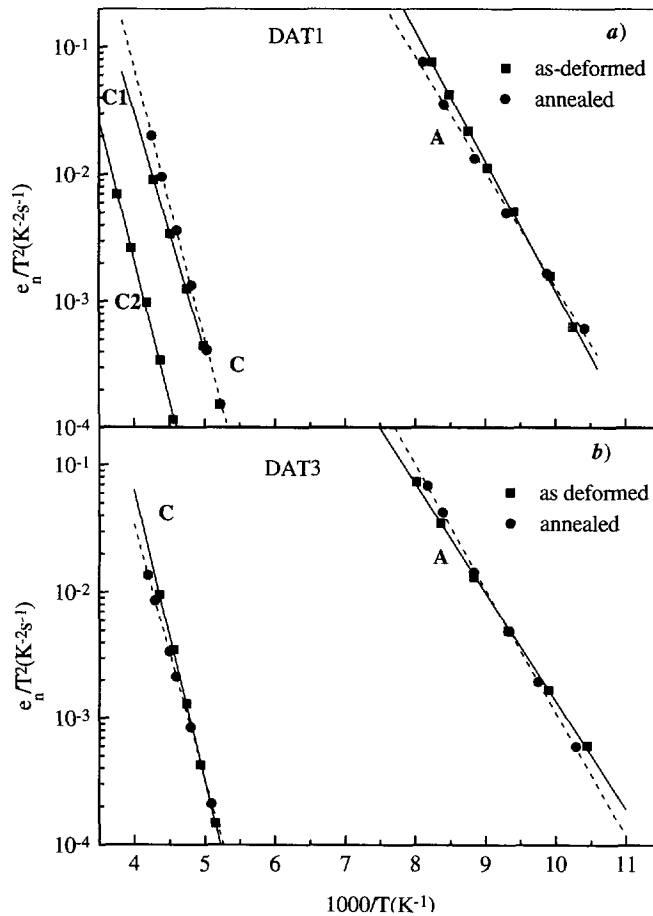


Fig 2. — Thermal emission rates (T^2 -corrected) as a function of inverse temperature for the traps A, C, C1 and C2 before (■) and after (●) annealing referring to a sample of the set DAT1 (a) and to a sample of the set DAT3 (b) The parameters of the lines A, C, C1 and C2 are reported in Table II

4. Discussion and Conclusions

The traps A and C survive after annealing, in both sets. The following characteristics must be noted: i) the peak amplitude of trap A remarkably decreases after annealing; ii) peak C, built up by two peaks in the samples deformed at 650 °C, reduces to one broad peak in annealed samples, and the concentration of the associated trap, strongly decreases after annealing in DAT1 samples. Furthermore this level is associated with a time dependent potential barrier whose asymptotic value is 0.23 eV. We can conclude that traps A and C are not associated with the same defect: the potential barrier associated with trap C induces a band bending that would shift, above the Fermi level, possible levels shallower than C and lying at the same place, which hence would be undetectable by DLTS. Trap A could be identified [2, 4] with point defect clusters related to dislocation motion. Trap C has been attributed [2] to defects located at the dislocations and its survival after annealing once more confirm this conclusion. The effect of the annealing on the shape of the peak, *i.e.* its reduction from a double line to a single broad line can be explained as follows. In Figure 4 the thermal emission rate

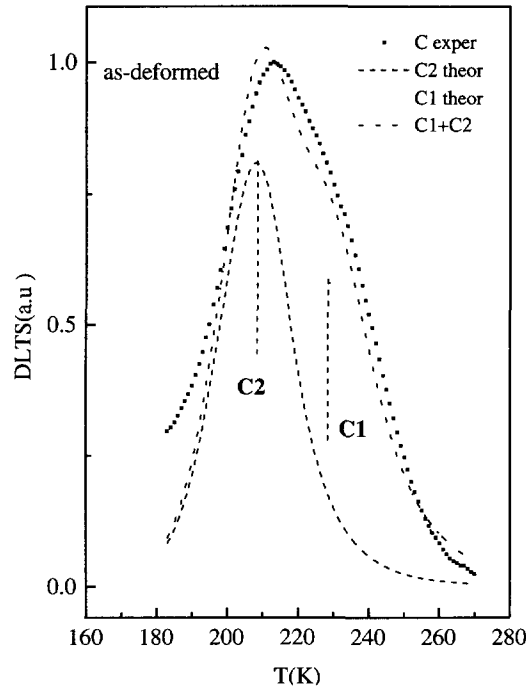


Fig. 3. — Experimental spectra of the line C in the set DAT1: line C (■) is given by the sum of two contributions C1(···) and C2 (- - -). Reverse bias and filling pulses are the same as in Figure 1.

Table II. — Results of DLTS investigations of trap C in as-deformed and annealed samples of the sets DAT1 and DAT3 obtained by fitting DLTS spectra and from the Arrhenius plot. E_a is the activation enthalpy, A_{pf} the prefactor defined as: $A_{pf} = \sigma_n \langle \nu_{th} \rangle \times \exp\left(\frac{\Delta S}{k}\right)$ where $\langle \nu_{th} \rangle$ and N_{CB} are thermal velocity and density of states in the conduction band, respectively, σ_n majority carrier capture cross-section, ΔS change in entropy due to the emission of one electron from the deep level to the conduction band and k Boltzmann constant.

Sample	Treatm.	E_a (eV)		A_{pf} (s^{-1})	
		Fit	Arrh	Fit	Arrh
DAT1	as-def C1	0.37 ^{a)}	0.37	8.1×10^5	9.3×10^5
	as-def C2	0.43 ^{a)}	0.43	4.0×10^7	1.2×10^6
	annealed	0.39	0.42	2.2×10^7	2.6×10^7
DAT3	as-def	0.43	0.45	2.0×10^7	9.8×10^7
	annealed	0.43	0.40	1.2×10^8	3.8×10^6

a) Obtained from deconvolution (see Fig. 3).

($-T^2$ corrected) of the levels C1, C2 and C referring to the present paper, are plotted *vs.* inverse temperature together with literature results. Notwithstanding a large scatter in the values of activation enthalpies given by different authors, by comparing the “fingerprints” of these traps, two different groups of lines could be identified. The level C could be included in the C1 group, as confirmed also by the results of the fitting procedure shown in Table II. As

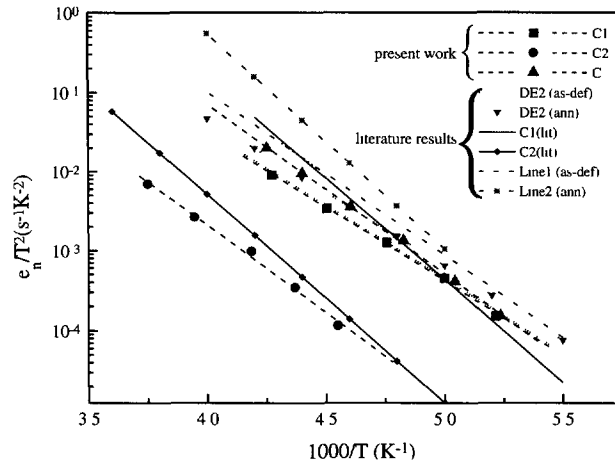


Fig. 4. — Comparison of thermal emission rates (T_2 -corrected) as a function of inverse temperature for the traps C1(■), C2(●) and C(▲) of the present work, with literature results: DE2: reference [6]; C1(lit), C2(lit): reference [4]; Line1 and Line2: reference [6]

the levels C1 and C2 have very similar activation enthalpies but different prefactors, they are attributed [4] to the same defect that could be located in different surroundings of the crystal. According with this hypothesis the trap C2 could be related to point defect clusters located in close proximity to the dislocations, while C1 could be due to the same defect cluster localized at the dislocations. Some of the defects responsible for C2 would anneal out during annealing, while others would move towards the dislocations contributing to the centres responsible for C1. This hypothesis would explain the disappearance of line C2 and the broadening of line C. Indeed, the resulting trap C corresponds to the trap C1, but with larger prefactor (*i.e.* with larger capture cross section), and becomes broadened due to the increase in the crystal disorder in its surroundings [7].

References

- [1] Peaker A.R. and Sidebotham E.C., Dislocation-related deep levels in silicon, in Properties of Silicon, EMIS Data Review, (INSPEC, London, 1988) p. 221 and reference therein.
- [2] Cavalcoli D., Cavallini A. and Gombia E., Energy levels associated with extended defects in plastically deformed n-type silicon, *J. Phys. III* (1997) 1399.
- [3] Cavalcoli D., Cavallini A. and Gombia E., Defect states in plastically deformed silicon, *Phys. Rev. B* **56** (1997) 10208.
- [4] Omling P., Weber E.R., Montelius L, Alexander H. and Michel J., Electrical properties of dislocations and point defects in plastically deformed silicon, *Phys. Rev. B.* **32** (1985) 6571.
- [5] Kveder V.V., Ossipyan Yu.A., Schroeter W. and Zoth G., On the energy spectrum of dislocations in silicon, *Phys. Stat. Sol. (a)* **72** (1982) 701.
- [6] Kronewitz J. and Schroeter W., Capacitance transient spectroscopy of 60°-dislocations in silicon, *Izvest Acad Nauk USSR Ser. Fiz.* **51** (1987) 682.
- [7] Kisielowski C. and Weber E.R., Inhomogeneities in plastically deformed silicon single crystals. I. ESR and photo-ESR investigations of p- and n-doped silicon, *Phys. Rev. B* **44** (1991) 1600.